Ab-initio calculation of state-resolved cross sections and rate coefficients for electron-oxygen scattering

V. Laporta
Istituto di Nanotecnologia, CNR, Bari (Italy)

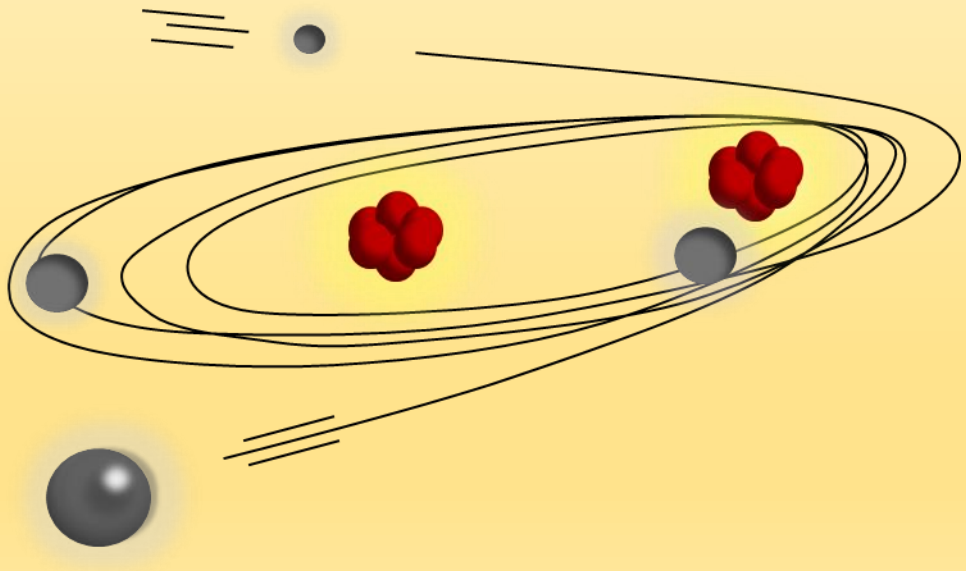

Workshop on Oxygen Plasma Kinetics
September 19 - 20, 2016, Reykjavik, Iceland

Plan of the talk:

- Short introduction to the theoretical formalism for electron-molecule resonant scattering;

- State-resolved cross sections database for electron-oxygen scattering
  - *Ab-initio* electron-O2(X,*v*) cross sections;
  - Cross sections for $^1\Delta$, $^1\Sigma$ excited states of oxygen;

- Applications
  - Electron-vibration relaxation in oxygen plasmas;
  - Non-equilibrium model for inductively coupled plasmas discharges;

Some theoretical details

Let's consider electron-molecule scattering with the presence of two (or more) interacting resonances:

$$
\begin{aligned}
e^- + AB(v) \rightarrow AB_1{}^-, AB_2{}^- &\rightarrow e^- + AB^*(w) && (VE)\\
&\rightarrow A^- + B && (DA)\\
&\rightarrow e^- + A + B && (DE)\\
e^- + AB^+(v) \rightarrow AB_1, AB_2 &\rightarrow A + B && (DR)
\end{aligned}
$$

The process can be described by two (or more) discrete electronic states, $|d_1\rangle$ and $|d_2\rangle$, *embedded-in* and *interacting-with* a single electronic continuum $|\vec{k}\rangle$

$$|\Psi\rangle \sim |d_1\rangle + |d_2\rangle + |\vec{k}\rangle$$

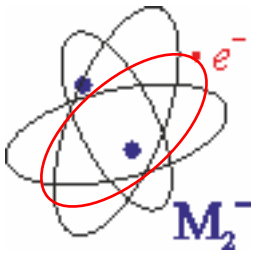

Resonant bound state

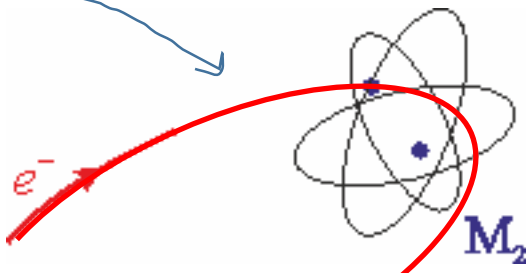

Interaction between electron and neutral molecule

The theory is developed in the *projector-operators* formalism within Hilbert space:

$$P = \int d\vec{k}\ |\vec{k}\rangle\langle\vec{k}|\,, \qquad Q = |d_1\rangle\langle d_1| + |d_2\rangle\langle d_2|$$

$$P + Q = 1\,, \qquad P^2 = P\,, \qquad Q^2 = Q\,, \qquad PQ = QP = 0$$

The electron-molecule effective Hamiltonian $H = H_0 + U + V$ can be written as:

$$H_0 = |d_1\rangle(T_N + V_0 + \epsilon_1)\langle d_1| + |d_2\rangle(T_N + V_0 + \epsilon_2)\langle d_2| + \int d\vec{k}\ |\vec{k}\rangle(T_N + V_0 + \epsilon_{\vec{k}})\langle\vec{k}|$$

$$U = |d_1\rangle U_{12}\langle d_2| + \text{h.c.}$$

$$V = \int d\vec{k}\ |d_1\rangle V_{1k}\langle\vec{k}| + |d_2\rangle V_{2k}\langle\vec{k}| + \text{h.c.}$$

- V_0 is the neutral molecule potential with eigenvalues equation:

$$(T_N + V_0)|v\rangle = \epsilon_v|v\rangle$$

- $\epsilon_{1,2}$ are the resonance positions respect to V_0
- *U* describes the coupling between the discrete states
- *V* couples the discrete states with the continuum states

Schrödinger equation for electron-molecule scattering. Ψ is the complete wave function of the system with total energy $E = \epsilon_{\vec{k}} + \epsilon_v$:

$$(H - E)|\Psi\rangle = 0$$

Splitting $|\Psi\rangle = \mathrm{P}|\Psi\rangle + \mathrm{Q}|\Psi\rangle$ into P e Q Hilbert subspace and projecting the Schrödinger equation, it obtains Lippmann-Swinger like equations for open-channel and closed-channel:

$$P(H_0 + U - E)P|\Psi\rangle = -PVQ|\Psi\rangle$$
$$Q(H_0 + U - E)Q|\Psi\rangle = -QVP|\Psi\rangle$$

Treating *V* as a perturbation the open-channel solution can be written as:

$$P|\Psi\rangle = P|\epsilon_{\vec{k}}\rangle|v\rangle + \frac{1}{P(E - H_0 - U)P}PVQ|\Psi\rangle$$

The homogeneous solution represents asymptotically a free electron $|\epsilon_{\vec{k}}\rangle$ and a target molecule in vibrational level $|v\rangle$

By putting the open-channel solution into closed-channel equation, after some manipulations, one has the final vector equation for the two resonant wave functions $\vec{\xi}(R) = (\xi_1, \xi_2)$:

$$\left(\hat{\mathcal{H}} - E\right)\vec{\xi}(R) + \int dR'\ \hat{K}(R, R', E)\vec{\xi}(R') = -\vec{V}_k\ \chi_v(R)$$

where $\vec{V}_k = (V_{1k}, V_{2k})$ are the coupling potentials and

$$\hat{\mathcal{H}} = \begin{pmatrix} T_N + V_1 & U_{12} \\ U_{21} & T_N + V_2 \end{pmatrix}$$

$$\hat{K}(R, R', E) = \sum_v \chi_v^*(R)\chi_v(R')\left[\hat{\Delta}(R, R', E - \epsilon_v) - \frac{i}{2}\hat{\Gamma}(R, R', E - \epsilon_v)\right]$$

$$\Gamma_{ij}(R, R', E - \epsilon_v) = 2\pi \int d\epsilon'\ V_{ik}\,\delta(E - \epsilon')\,V^*{}_{jk} \qquad i, j = 1,2$$

$$\Delta_{ij}(R, R', E - \epsilon_v) = \frac{1}{2\pi} P \int d\epsilon'\ \frac{\Gamma_{ij}(R, R', \epsilon')}{E - \epsilon_v - \epsilon'} \qquad i, j = 1,2$$

The nuclear dynamics, in the full theory, is governed by *complex*, *non-local* and *energy-dependent* operators.

The local approximation (the so-called 'boomerang model') of the full theory consists to make the following two *ansatz* in the kernel $\widehat{K}$:

(spacing of the vibrational levels)

$$\text{If } |v_n - v_m| \ll \epsilon_{\vec{k}} \quad \forall\, n, m \quad \Longrightarrow \quad E - v_n = \epsilon_{\vec{k}} + v_i - v_n \approx \epsilon_{\vec{k}}$$

(resonance positions)

$$\epsilon_{\vec{k}} \simeq \epsilon_1(R) = V_1(R) - V^0(R)$$
$$\epsilon_{\vec{k}} \simeq \epsilon_2(R) = V_2(R) - V^0(R)$$

With these replacements the kernel $\widehat{K}$ become *local* (=dependent on just one geometry) and *energy-independent*.

$$\left[\begin{pmatrix} T_N + V_1 & U_{12} \\ U_{21} & T_N + V_2 \end{pmatrix} - \frac{i}{2}\hat{\Gamma}(R) - E\widehat{\mathbf{1}}\right]\vec{\xi}(R) = -\vec{V}_k\, \chi_v(R)$$

The final resonant vibrational-excitation cross section for transition $v_i \rightarrow v_f$ and for electron energy ϵ is given by:

$$\sigma_{i,f}(\epsilon) = \frac{2s_r + 1}{2(2s+1)} \frac{g_r}{g} \frac{64\pi^5 m^2}{\hbar^4} \frac{k_f}{k_i} |T_{11} + T_{22} + T_{12} + T_{21}|^2$$

where the *T* matrix elements are given by

$$T_{pq} = \left\langle \chi_f \middle| V_{pk_f} \middle| \xi_q \right\rangle \qquad p, q = 1,2$$

For a two <u>non-interacting</u> resonances the cross section reduces to:

$$\sigma_{i,f}(\epsilon) = \frac{2s_r + 1}{2(2s+1)} \frac{g_r}{g} \frac{64\pi^5 m^2}{\hbar^4} \frac{k_f}{k_i} (|T_{11}|^2 + |T_{22}|^2)$$

The corresponding rate coefficient, assuming for electrons a Maxwell distribution at temperature *kT,* is given by:

$$K_{i,f}(T) = \frac{2}{\sqrt{\pi}} (kT)^{-1.5} \int d\epsilon \; \epsilon \, \sigma_{i,f}(\epsilon) \, e^{-\epsilon/kT}$$

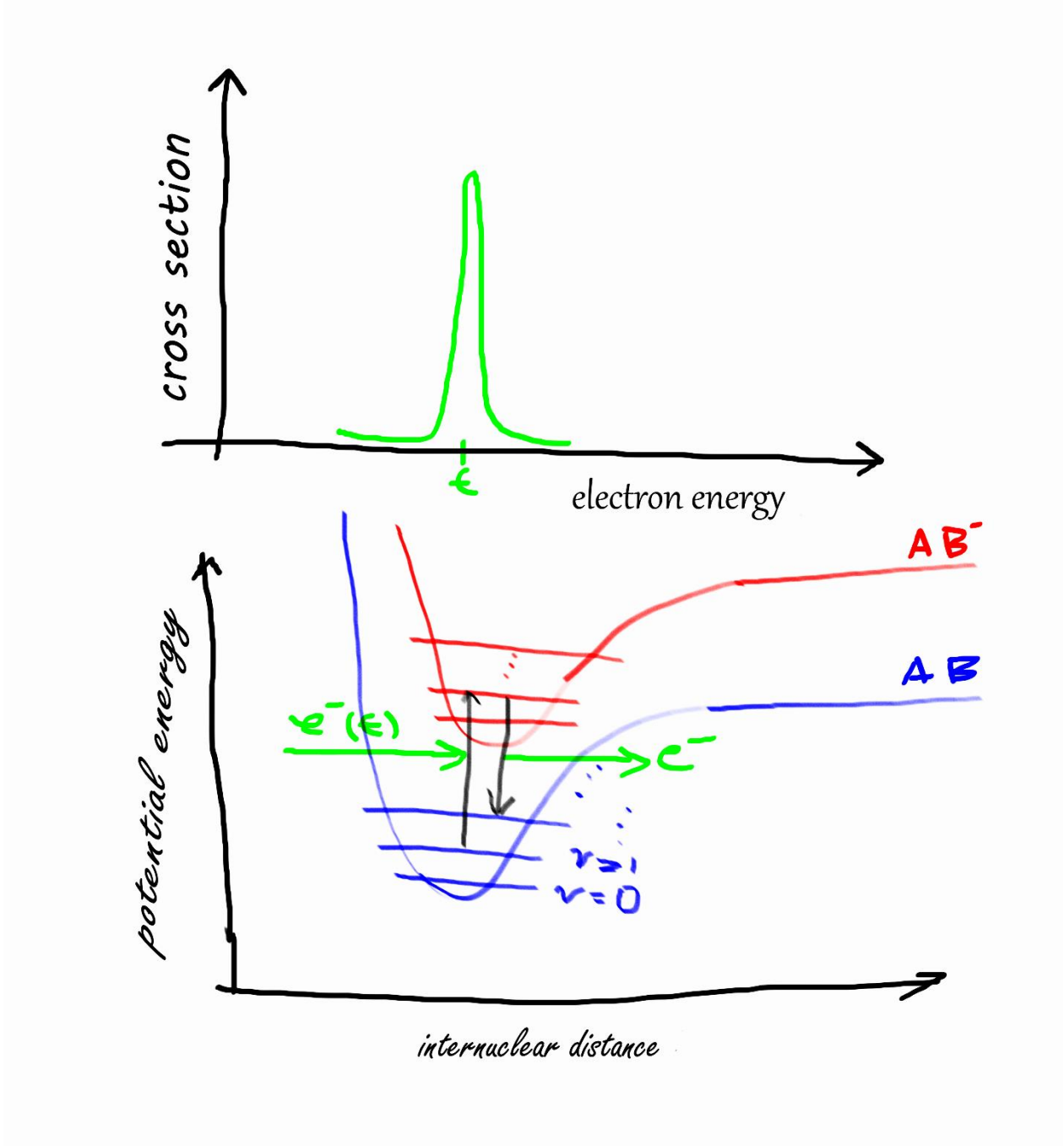

Resonant
Vibrational-excitation
cross section

$e^- + AB(v) \rightarrow AB^- \rightarrow AB(v') + e^-$

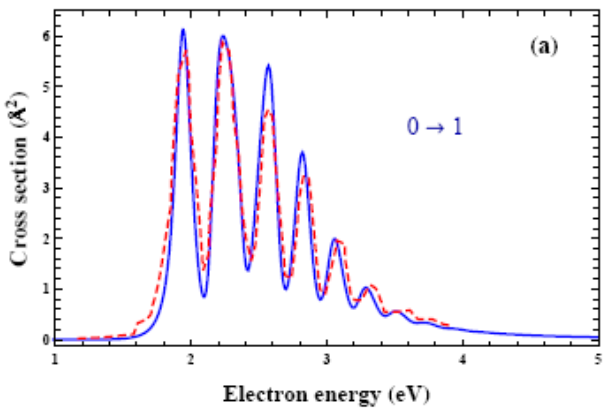

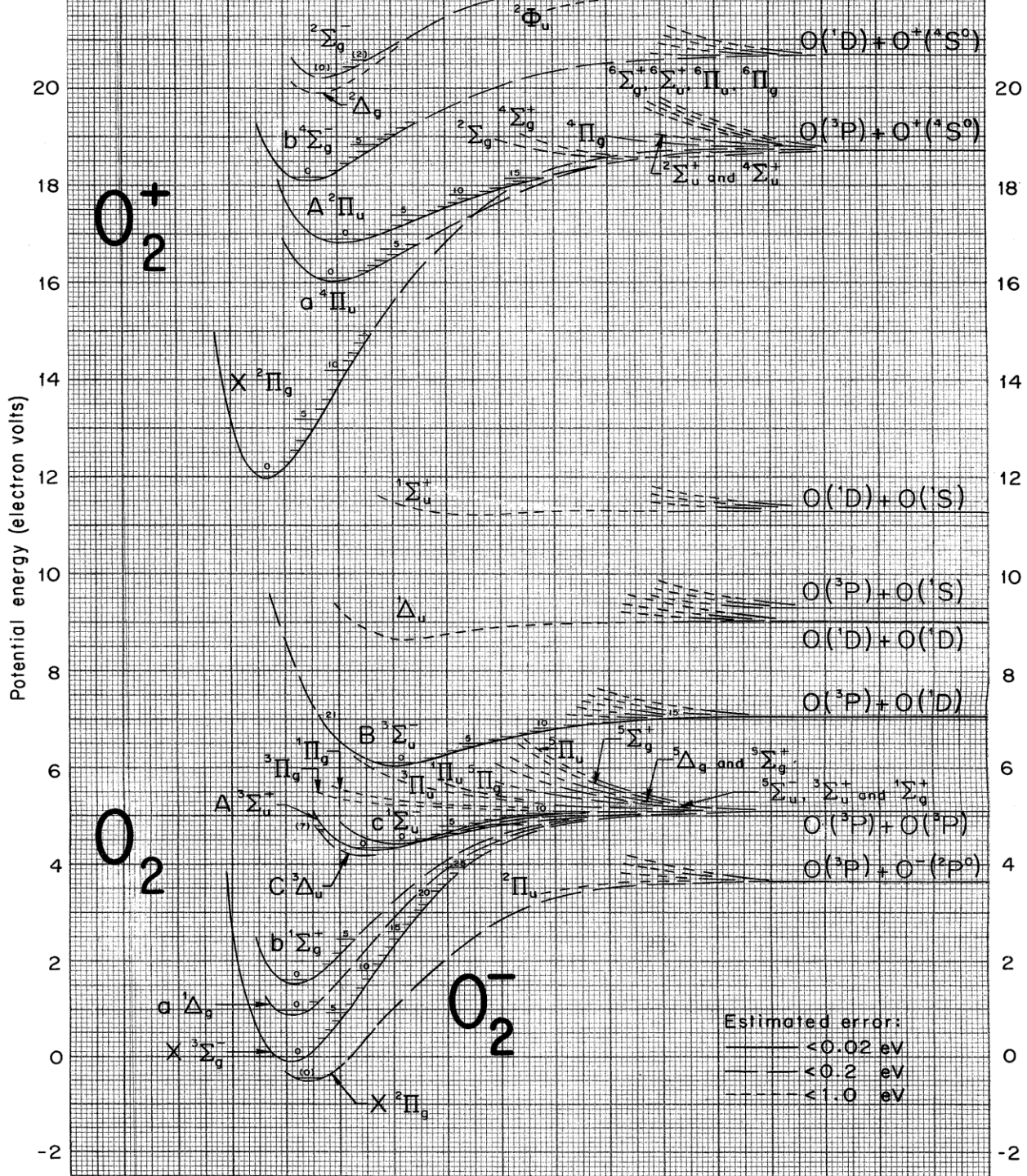

State-resolved
cross sections database
for
electron-oxygen
scattering

electron-O_2(X, v) resonant scattering

In order to describe the low-energy electron-O_2($X\ ^3\Sigma_g^-$) resonant scattering it needs to include four resonant states, $^2\Pi_g$, $^2\Pi_u$, $^4\Sigma_u^-$, $^2\Sigma_u^-$ of O_2^-.

Potential energy curves and resonance widths obtained from MOLPRO and R-matrix within aug-cc-pvQZ basis-set and MR-CI model.

The O_2 target was represented using the corresponding orbital configurations: 3 core orbitals $(2a_g, 1b_{1u})^6$ of frozen electrons and 9 valence orbitals up to $(3a_g, 2b_{3u}, 2b_{2u}, 3b_{1u}, 1b_{2g}, 1b_{3g})^{10}$.

For the scattering calculations:
$(2a_g, 1b_{1u})^6$ $(5a_g, 2b_{3u}, 2b_{2u}, 4b_{1u}, 2b_{2g}, 2b_{3g})^{11}$ and
$(2a_g, 1b_{1u})^6$ $(5a_g, 2b_{3u}, 2b_{2u}, 4b_{1u}, 2b_{2g}, 2b_{3g})^{10}$ $(6a_g, 3b_{3u}, 3b_{2u}, 1b_{1g}, 5b_{1u}, 3b_{2g}, 3b_{3g}, 1a_u)^1$.

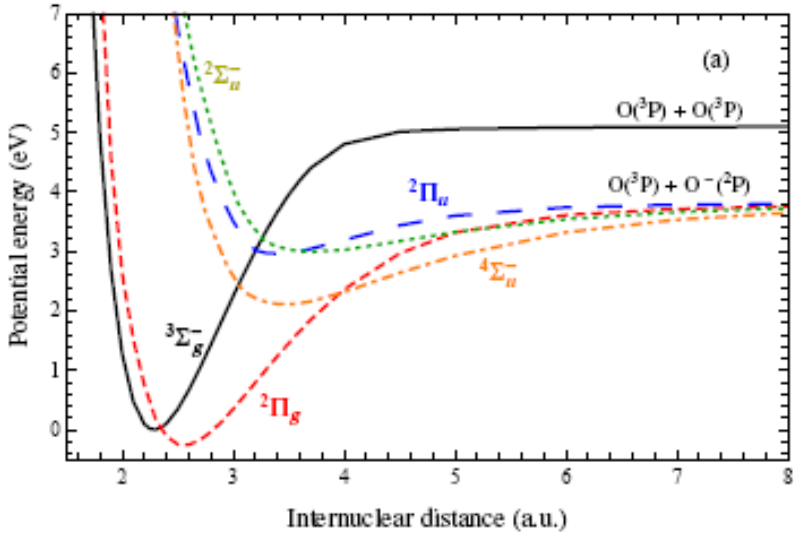

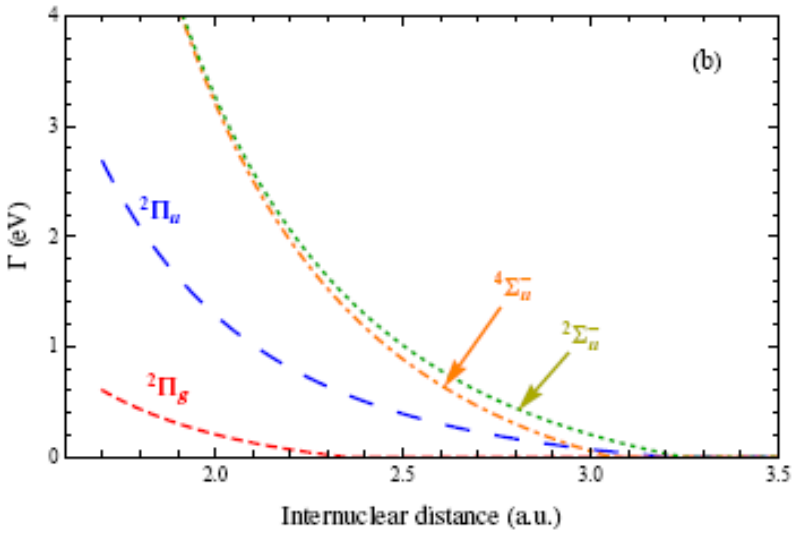

Table 1. Reduced mass (μ), dissociation energy (D_e) and equilibrium distance (R_e) for O_2 and O_2^- potentials. Electron affinity (eA) of O_2 and the crossing point (R_c) between the O_2 and O_2^- potential energy curves are also given. Literature values, where available, are given in parentheses.

	$O_2(X\,^3\Sigma_g^-)$	O_2^-			
		$^2\Pi_g$	$^2\Pi_u$	$^4\Sigma_u^-$	$^2\Sigma_u^-$
μ (a.u.)	14582.6				
D_e (eV)	5.10 (5.12 [20])	4.02	0.83	1.54	0.73
R_e (a.u.)	2.29 (2.28 [20])	2.55	3.38	3.47	3.73
R_c (a.u.)	—	2.34	3.20	3.03	3.25
eA (eV)	1.45 (1.46 [21])				

Table 1
Calculated vibrational levels of $O_2(X^3\Sigma_g^-)$ molecule for rotational level $j = 1$. Energies are given in eV.

v	ϵ_v	v	ϵ_v	v	ϵ_v
0	0.000	14	2.435	28	4.280
1	0.196	15	2.587	29	4.382
2	0.388	16	2.735	30	4.476
3	0.573	17	2.881	31	4.565
4	0.756	18	3.024	32	4.651
5	0.937	19	3.164	33	4.730
6	1.117	20	3.301	34	4.794
7	1.291	21	3.436	35	4.847
8	1.461	22	3.568	36	4.898
9	1.629	23	3.696	37	4.938
10	1.796	24	3.821	38	4.960
11	1.960	25	3.942	39	4.976
12	2.122	26	4.059	40	4.987
13	2.281	27	4.172	41	4.994

V. Laporta, R. Celiberto and J. Tennyson, *Phys. Rev.* ***A*****91**, 012701 (2015).
V. Laporta, R. Celiberto and J. Tennyson, *Plasma Sources Sci. Technol.* ***22****, 025001 (2013)*

Vibrational-Excitation process:

$$e^- + O_2(X\,^3\Sigma_g^-;\, v) \longrightarrow O_2^-(^2\Pi_g, ^2\Pi_u, ^4\Sigma_u^-, ^2\Sigma_u^-) \longrightarrow e^- + O_2(X\,^3\Sigma_g^-;\, v')$$

At energy below 2 eV the VE cross sections are dominated by $^2\Pi_g$ symmetry; comparison with Allan's results

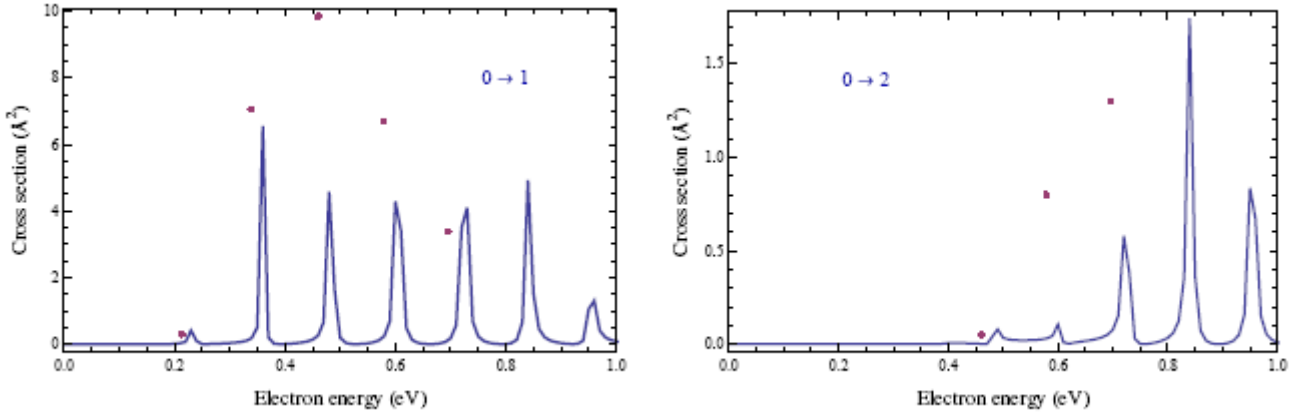

Resonance at 10 eV dominated by $^4\Sigma_u^-$ symmetry

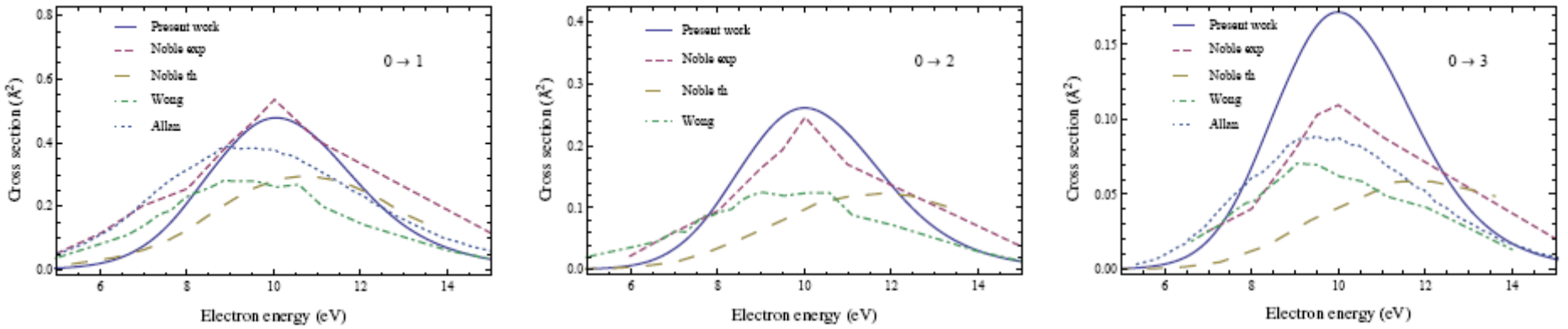

Set of calculated cross sections for $j = 1$

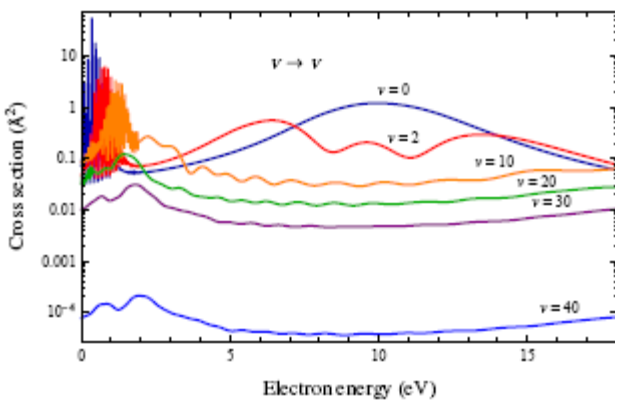

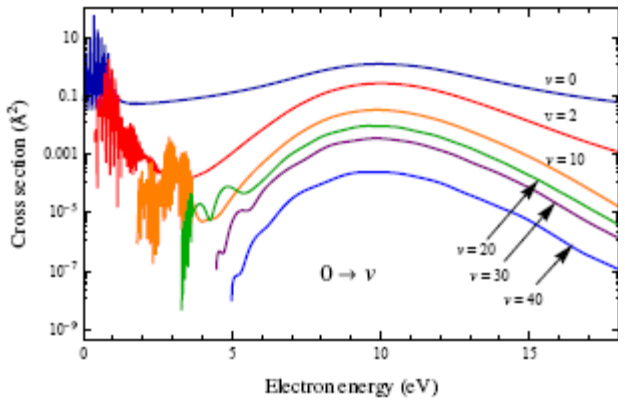

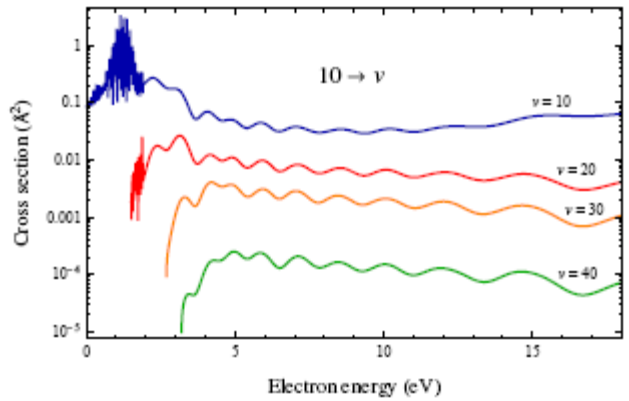

and the corresponding rate coefficients

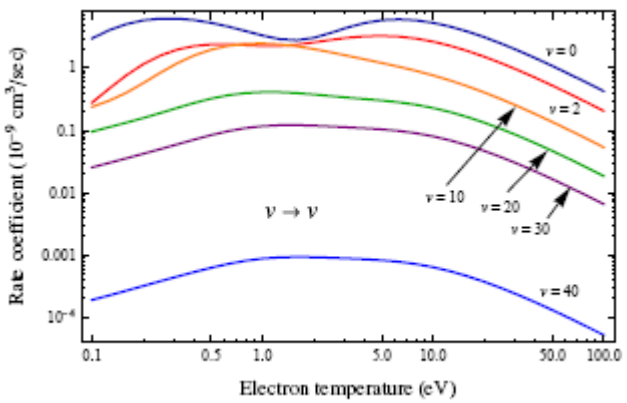

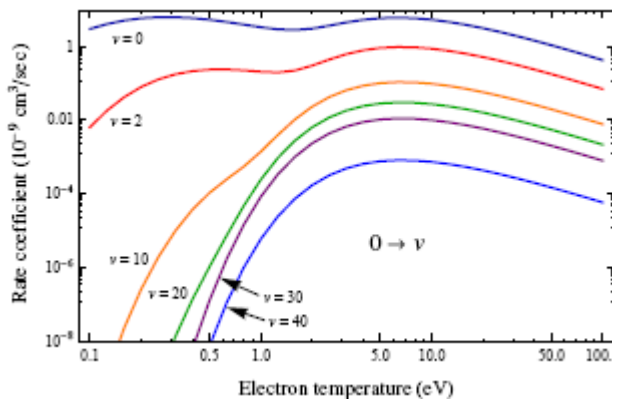

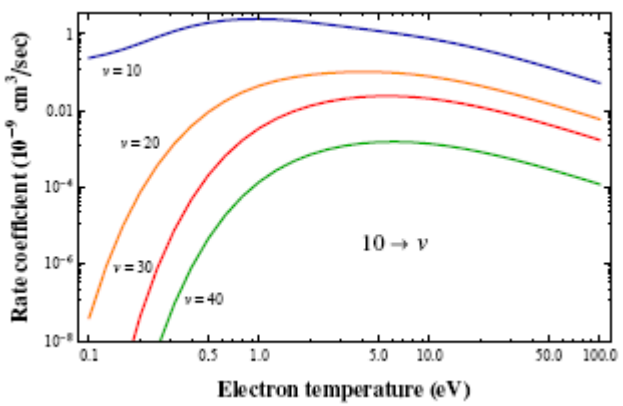

Dissociative-electron-attachment

$$e^- + O_2(X\,^3\Sigma_g^-;\, v) \longrightarrow O_2^-(^2\Pi_g, ^2\Pi_u, ^4\Sigma_u^-, ^2\Sigma_u^-) \longrightarrow O(^3P) + O^-(^2P)$$

DeA cross section for ***v* = 0** and ***j* = 1**
Contributions from the four symmetries and comparison with some theoretical and experimental data present in literature

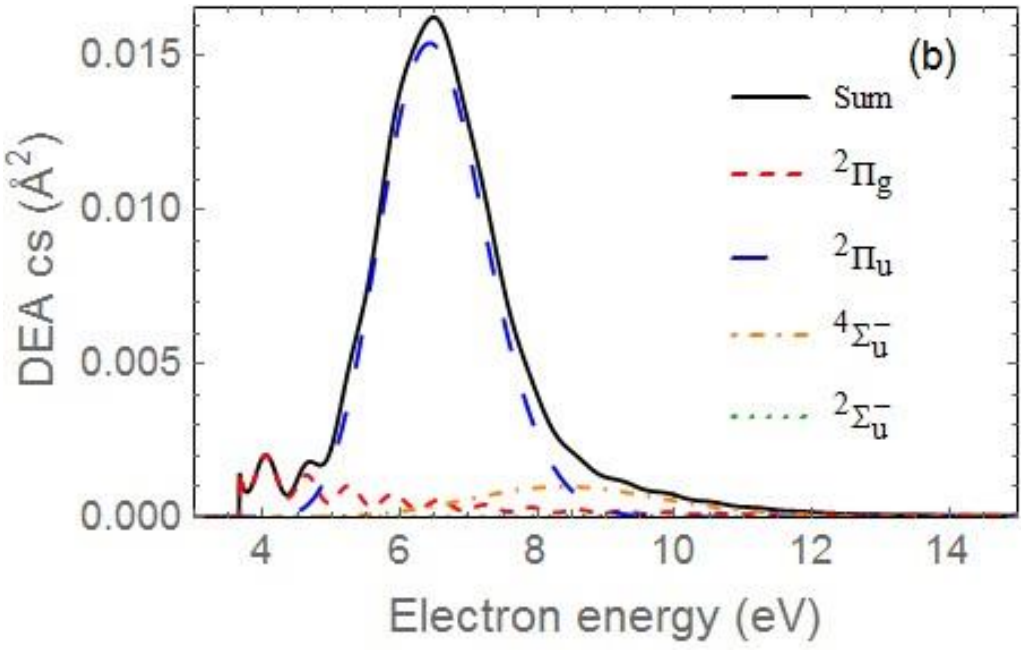

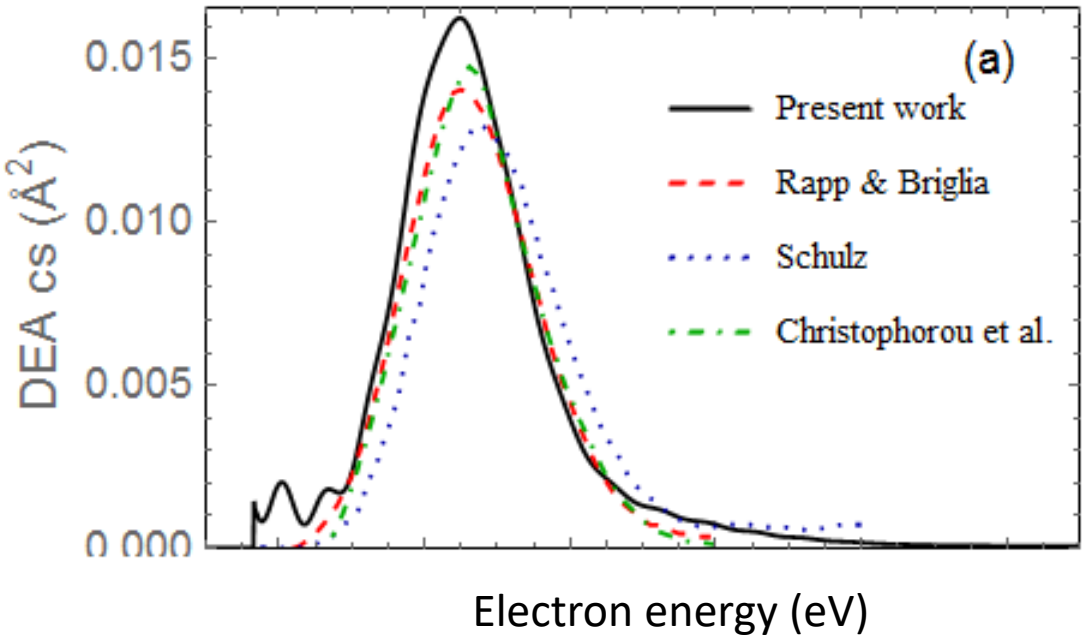

Set of calculated cross sections and the corresponding rate coefficients for some vibrational levels *v* and for *j* = 1

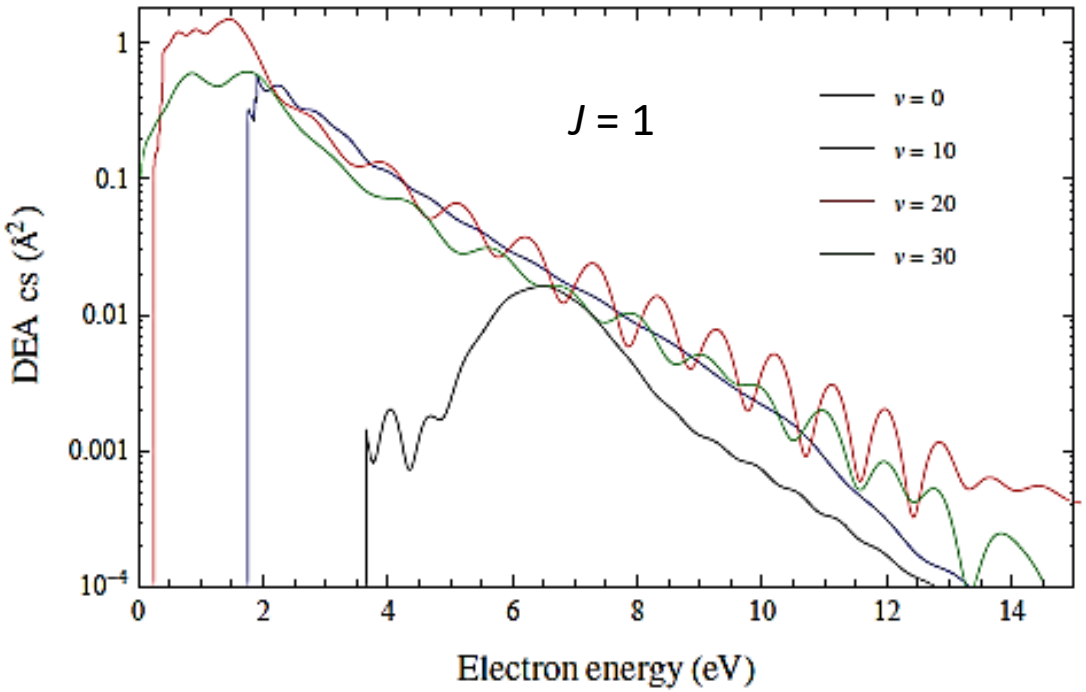

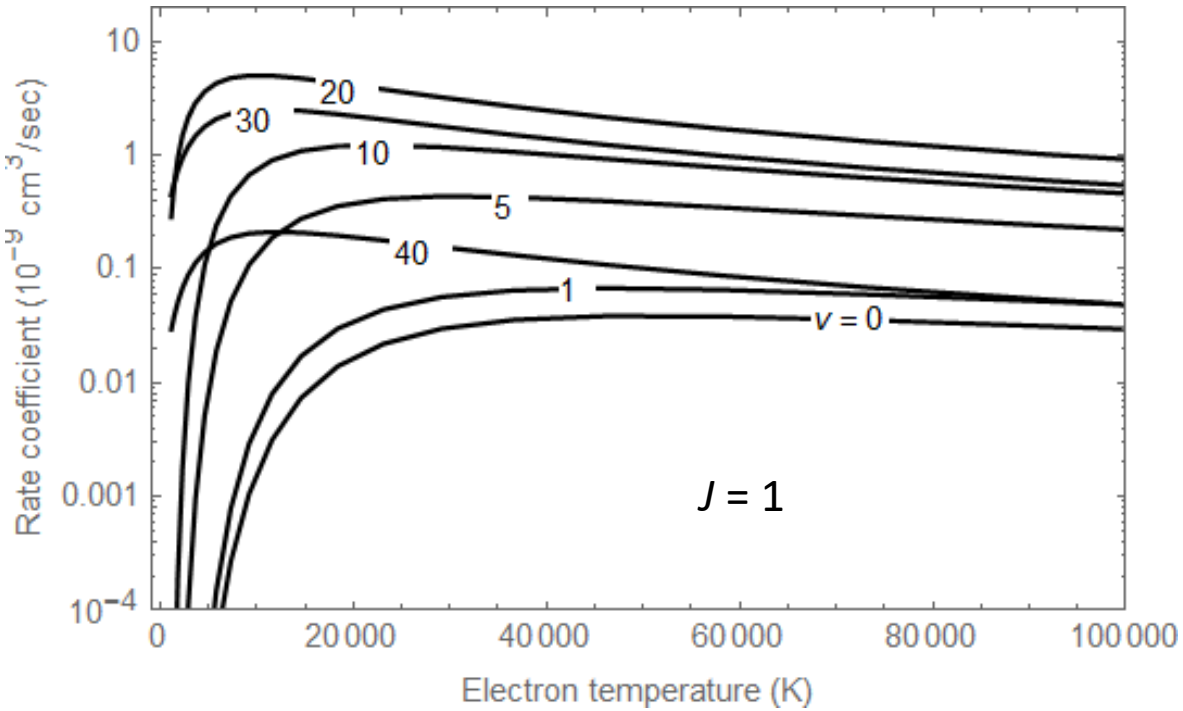

Electron-impact dissociation:

$$e^- + O_2(X^3\Sigma_g^-;\, v) \longrightarrow O_2^-(^2\Pi_g, ^2\Pi_u, ^4\Sigma_u^-, ^2\Sigma_u^-) \longrightarrow e^- + 2\,O(^3P)$$

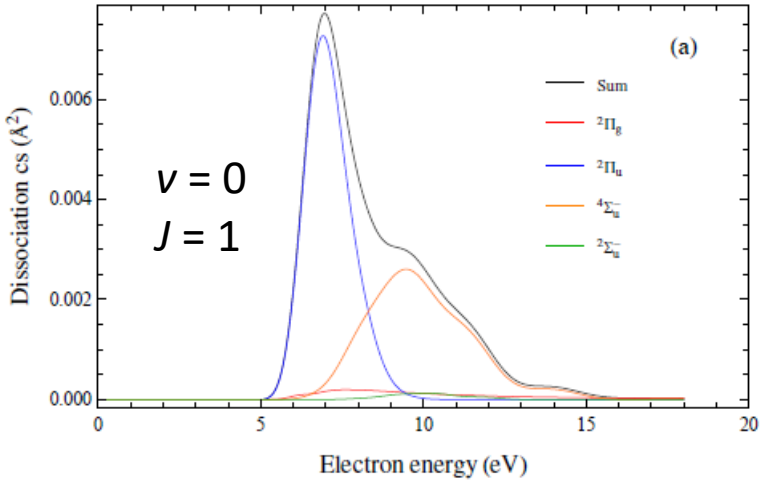

Set of vibrational-resolved cross sections and the corresponding rate coefficients for $j = 1$

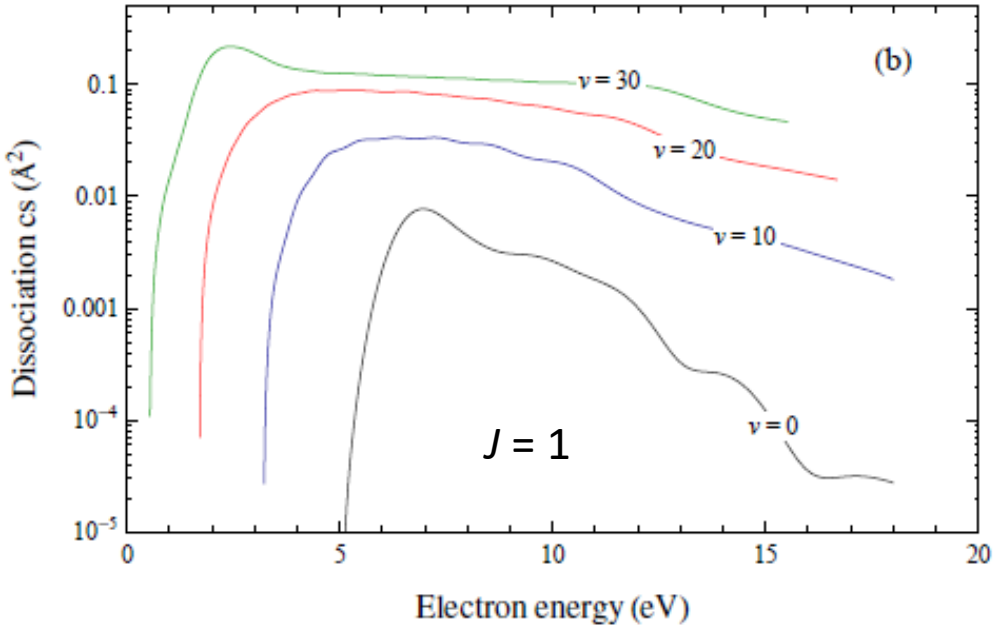

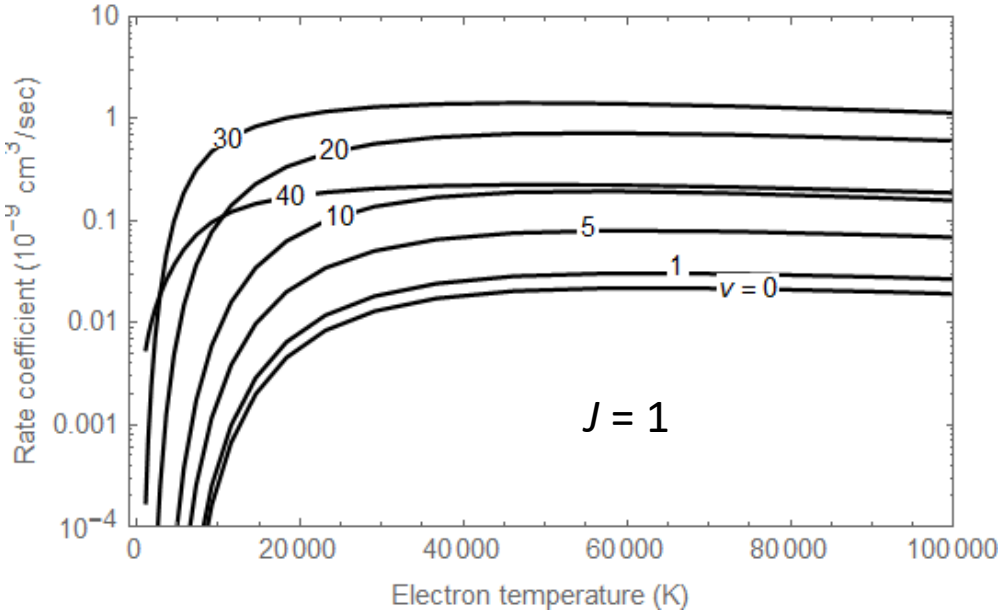

Effect of target rotation

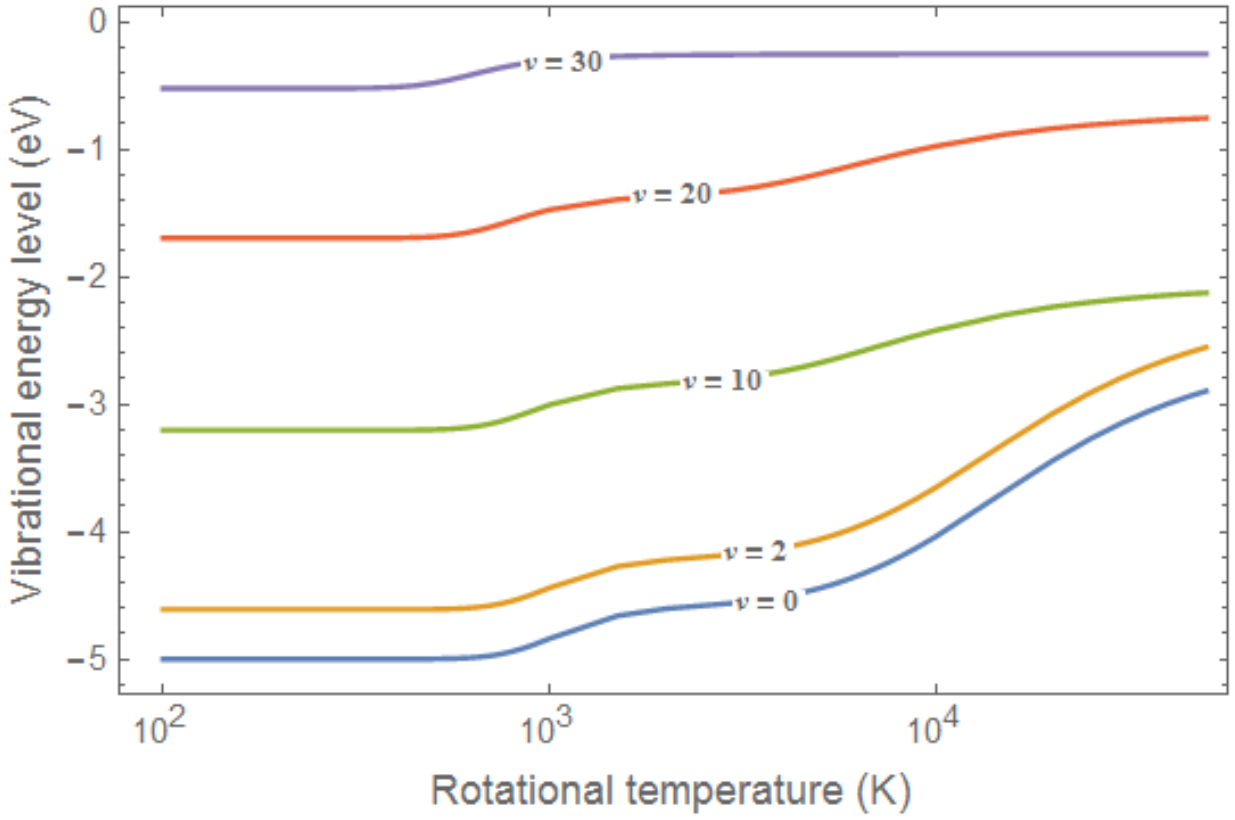

Number of vibrational levels as a function of the rotational quantum number *j*

$j = 1$	$v_1 = 0\ldots41$
$j = 50$	$v_{50} = 0\ldots33$
$j = 100$	$v_{100} = 0\ldots23$
$j = 150$	$v_{150} = 0\ldots9$
$j = 170$	$v_{170} = 0\ldots2$

Thermal averaged energy of the ro-vibrational level $\epsilon_{v,j}$:

$$\overline{\epsilon_v}(T_r) = \sum_j \epsilon_{v,j}(2j+1)\frac{e^{-\epsilon_{v,j}/k_B T_r}}{Q_v(T_r)}$$

T_r is the rotational temperature

Thermal averaged vibrational-excitation cross section, T_r is the rotational temperature:

$$\bar{\sigma}_{v,v'}(\epsilon, T_r) = \sum_j \sigma_{v,v',j}(\epsilon)(2j+1)\frac{e^{-\epsilon_{v,j}/k_B T_r}}{Q_v(T_r)}$$

j-resolved cross section for $v = 0 \rightarrow v' = 1$

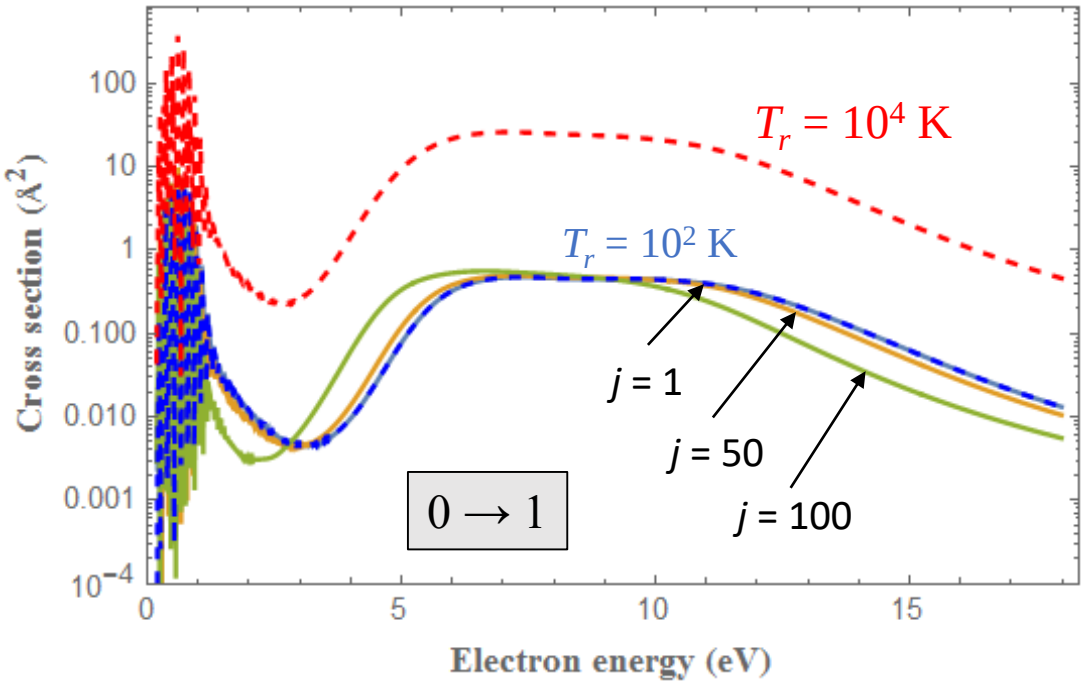

Thermal averaged rate coefficient by assuming the rotational temperature in equilibrium with electron temperature

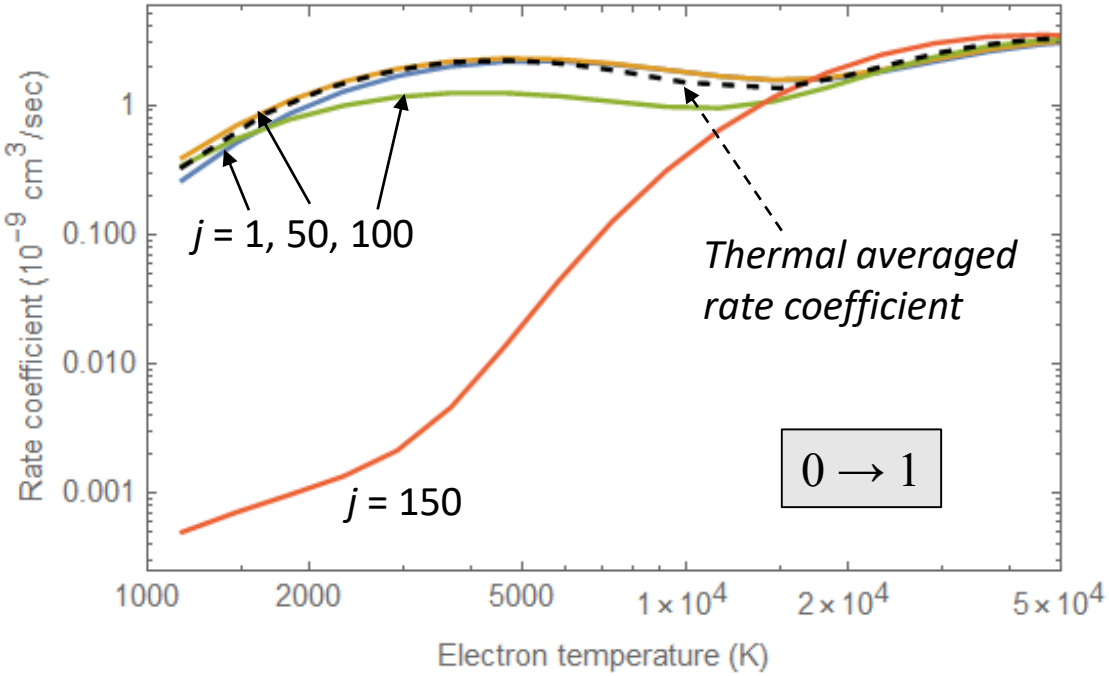

Rotational *j*-resolved rate coefficients (solid lines) for dissociative-electron-attachment and for dissociative-excitation processes for $v = 0$ as a function of the electron temperature

and

Thermal averaged rate coefficient (dashed line) for $v = 0$ by assuming the rotational temperature in equilibrium with electron temperature

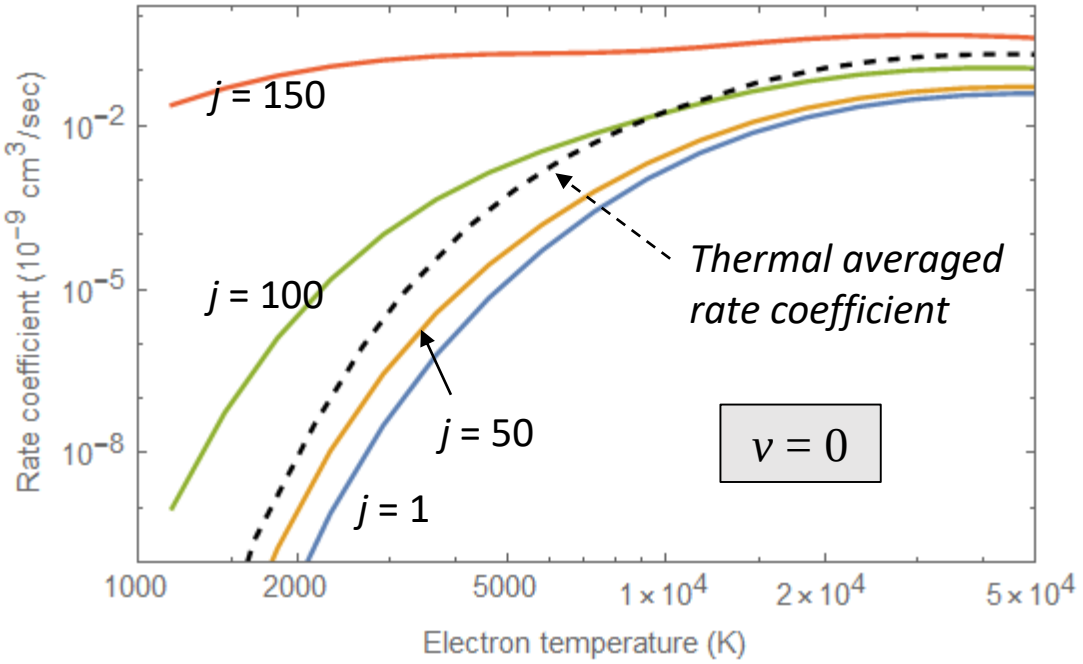

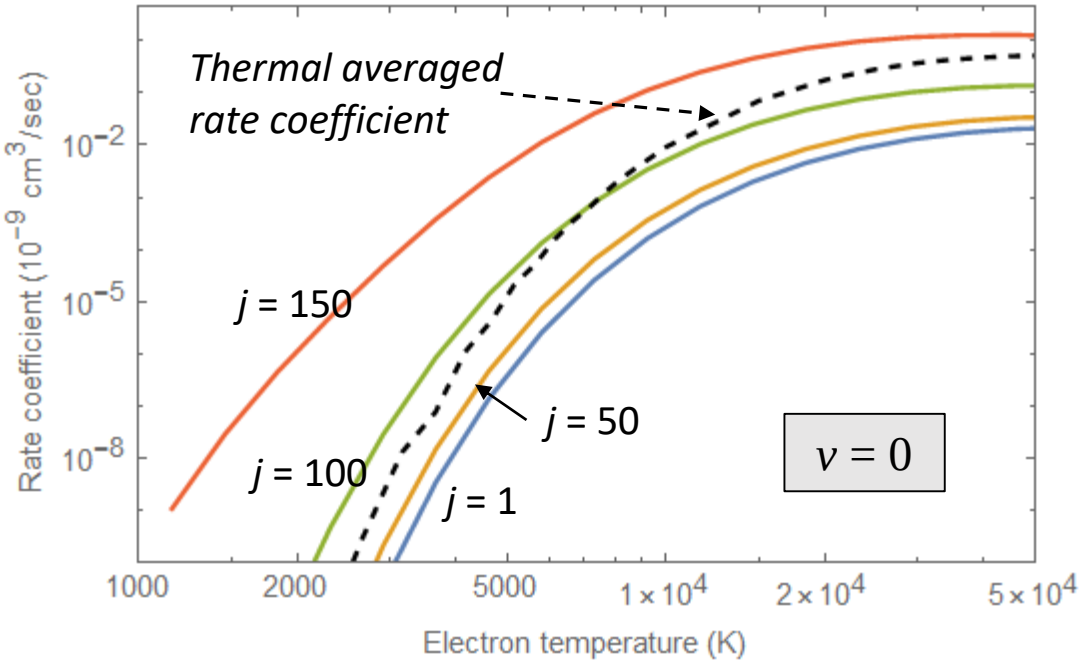

Cross sections for $^1\Delta$, $^1\Sigma$ excited states of oxygen*

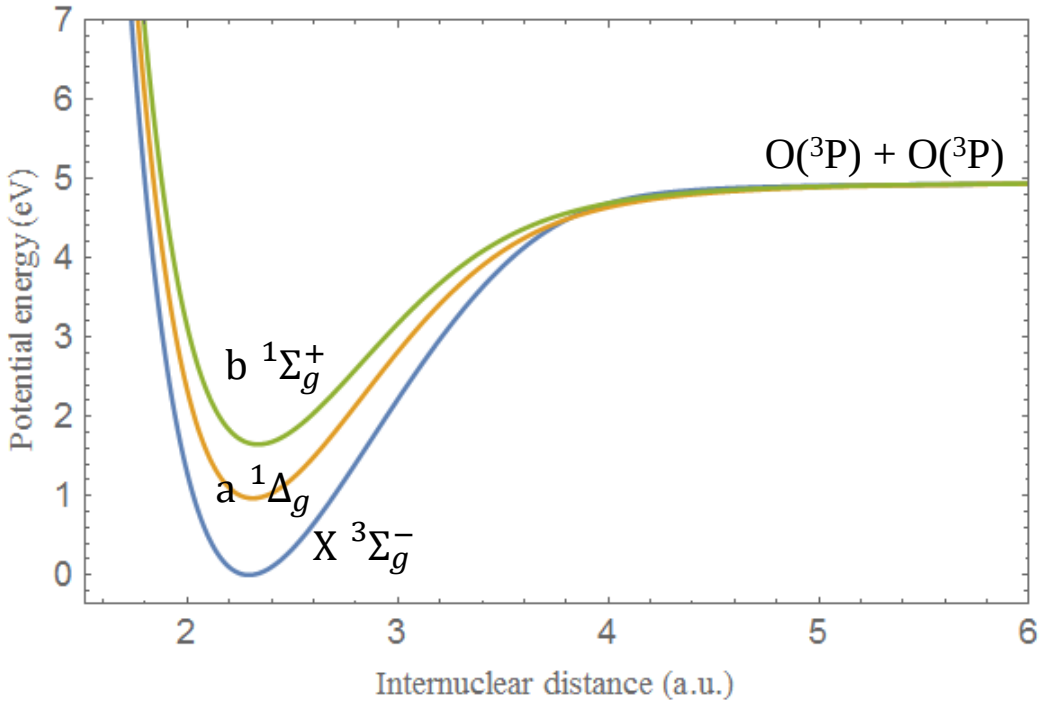

v	ϵ_v (eV) $O_2(X\,^3\Sigma, v)$	$O_2(a\,^1\Delta, v)$	$O_2(b\,^1\Sigma, v)$
0	0.0957	1.0588	1.7329
1	0.2861	1.2394	1.9026
2	0.4738	1.4168	2.0689
3	0.6586	1.5912	2.2318
4	0.8408	1.7624	2.3914
5	1.0202	1.9306	2.5475
6	1.1969	2.0955	2.7002
7	1.3709	2.2572	2.8493
8	1.5421	2.4156	2.9948
9	1.7106	2.5707	3.1365
10	1.8764	2.7224	3.2743
11	2.0394	2.8707	3.4082
12	2.1996	3.0153	3.5380
13	2.3570	3.1563	3.6635
14	2.5116	3.2935	3.7847
15	2.6633	3.4269	3.9013
16	2.8121	3.5562	4.0130
17	2.9580	3.6813	4.1198
18	3.1009	3.8020	4.2212
19	3.2407	3.9181	4.3170
20	3.3773	4.0294	4.4069
21	3.5107	4.1355	4.4906
22	3.6407	4.2363	4.5677
23	3.7672	4.3313	4.6378
24	3.8900	4.4203	4.7007
25	4.0088	4.5029	4.7561
26	4.1235	4.5787	4.8037
27	4.2336	4.6474	4.8435
28	4.3388	4.7088	4.8756
29	4.4386	4.7624	4.9006
30	4.5323	4.8084	4.9191
31	4.6190	4.8467	4.9324
32	4.6976	4.8776	4.9415
33	4.7667	4.9017	4.9475
34	4.8246	4.9198	4.9526
35	4.8692	4.9328	
36	4.8995	4.9416	
37	4.9181	4.9472	
38	4.9301	4.9527	
39	4.9389		
40	4.9449		
41	4.9499		

*Thanks to David Schwenke (NASA Ames (US)) for supplying the potential energy curves

- State-resolved cross sections can be obtained by splitting procedure from the global cross section;

- By setting $Y, Y' = \{\mathrm{X}\ ^3\Sigma_g^-, \mathrm{a}\ ^1\Delta_g, \mathrm{b}\ ^1\Sigma_g^+\}$ the excited states of O_2 and by *v, v'* the corresponding vibrational levels, in order to split the global cross section $\sigma_{Y'Y}^{exp}$ into vibrational-resolved cross section $\sigma_{Yv}^{Y'v'}$ the following formula can be used:

$$\sigma_{Yv}^{Y'v'}(\epsilon) = q_{Yv}^{Y'v'}\,\sigma_{Y'Y}^{exp}\left(\epsilon\,\frac{\Delta E_{Y0}^{Y'0}}{\Delta E_{Yv}^{Y'v'}}\right),$$

where ϵ is the electron energy,

$$q_{Yv}^{Y'v'} = \left|\left\langle \psi_{v'}^{Y'} \middle| \psi_{v}^{Y} \right\rangle\right|^2,$$

the Frank-Condon factor and

$$\Delta E_{Yv}^{Y'v'} = \left|\epsilon_{v'}^{Y'} - \epsilon_{v}^{Y}\right|,$$

is the threshold energy for the $Y, v \rightarrow Y', v'$ transition

Experimental global cross section for
$e + O_2(X, {}^1\Delta, {}^1\Sigma)$
Alves *et al.* Eur. Phys. J. D (2016) 70: 124

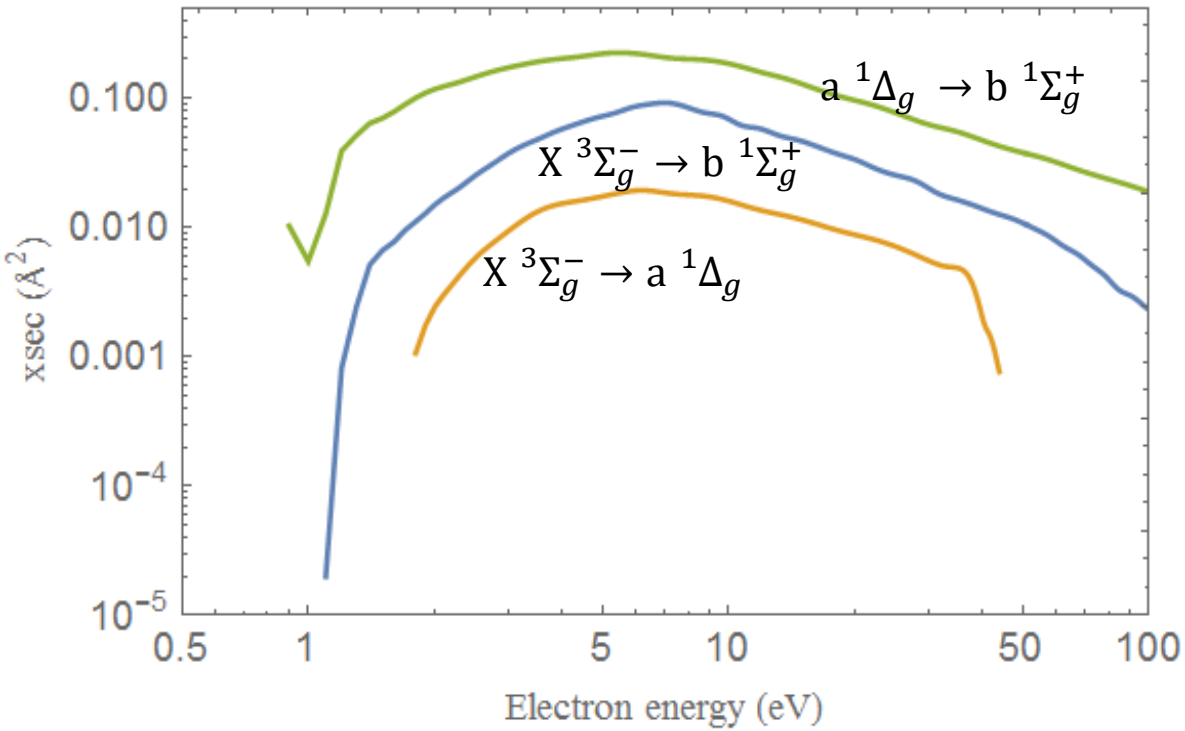

$X \rightarrow {}^1\Delta$ cross sections

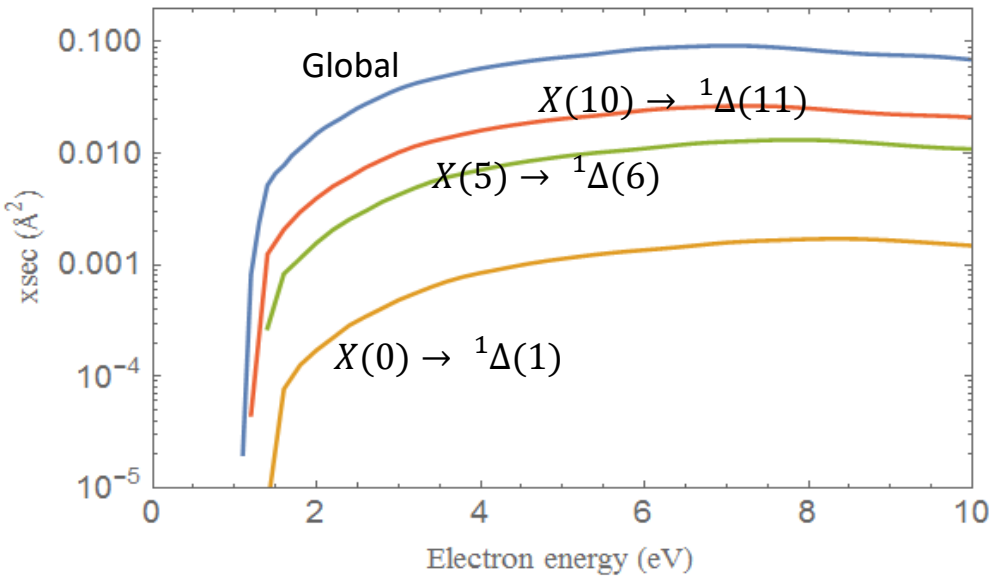

$X \rightarrow {}^1\Sigma$ cross sections

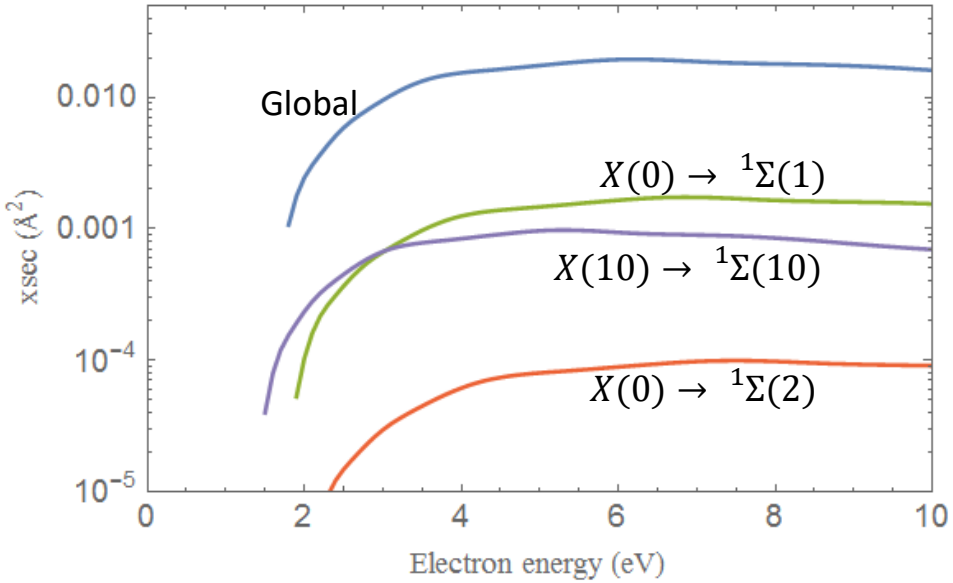

${}^1\Delta \rightarrow {}^1\Sigma$ cross sections

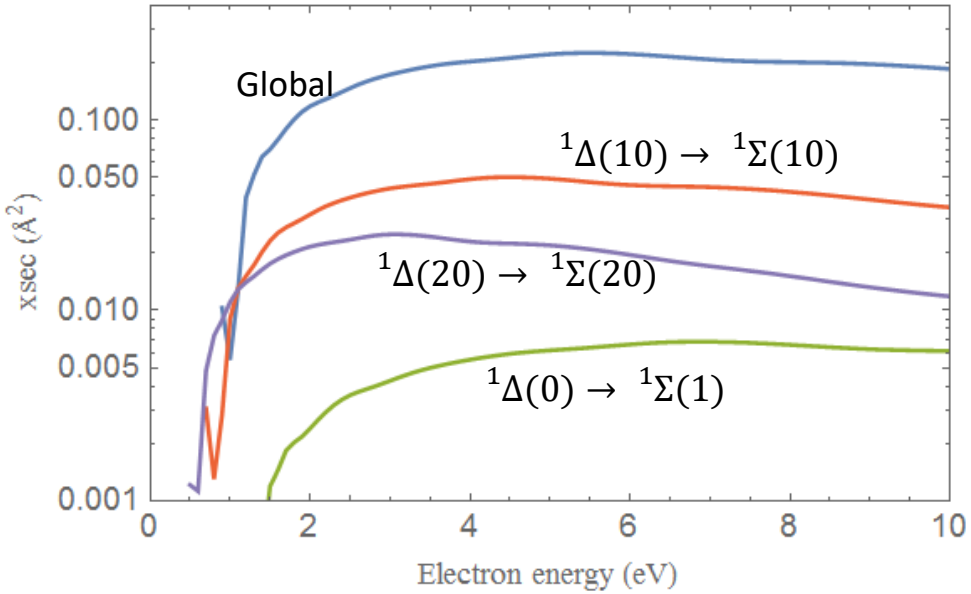

Application: Electron-vibration relaxation in oxygen plasmas

$$e + O_2(X\,^3\Sigma_g^-; v, j) \rightleftarrows e + O_2(X\,^3\Sigma_g^-; w, j), \quad \text{(VE)}$$

- State-to-State vibrational kinetics
- Vibrational relaxation time is comparable to chemical relaxation: vibrational non-equilibrium

$$\frac{dn_v}{dt} = n_e \sum_{w \in \mathcal{V}} [k_{w,v}\, n_w - k_{v,w}\, n_v], \qquad v \in \mathcal{V},$$

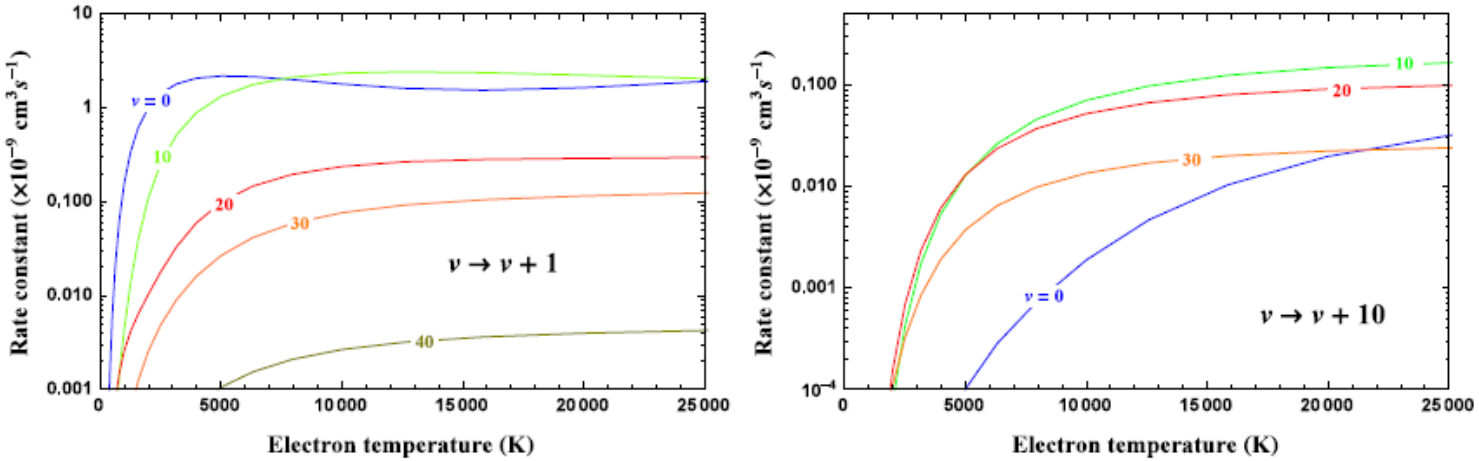

V. Laporta, K.L. Heritier and M. Panesi, Chemical Physics **472** (2016) 44–49

- Time evolution of non-equilibrium vibrational distribution function:

Equilibrium distribution

Non-equilibrium distribution

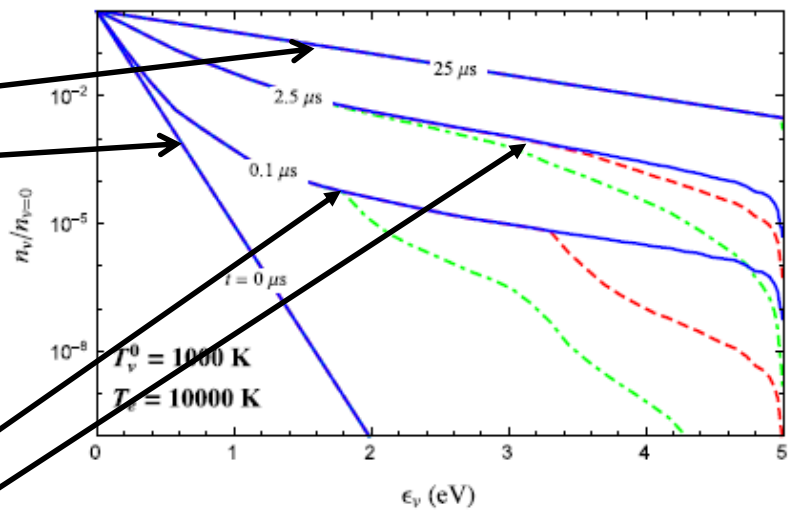

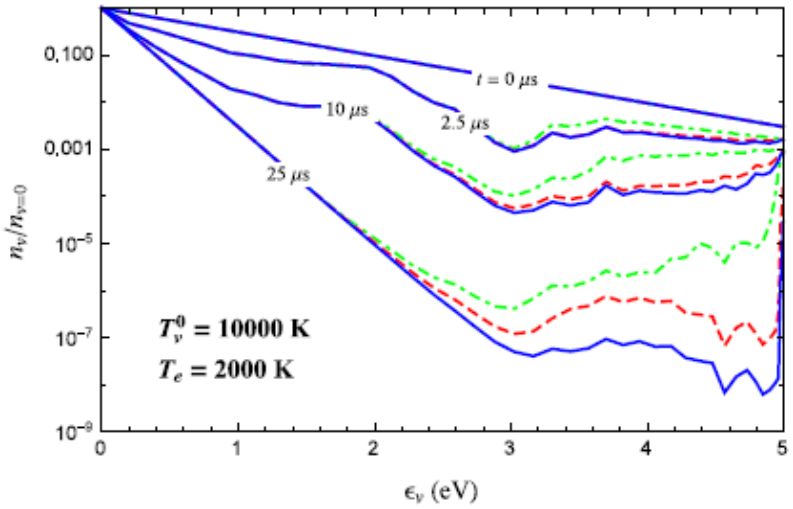

- Vibrational relaxation time:

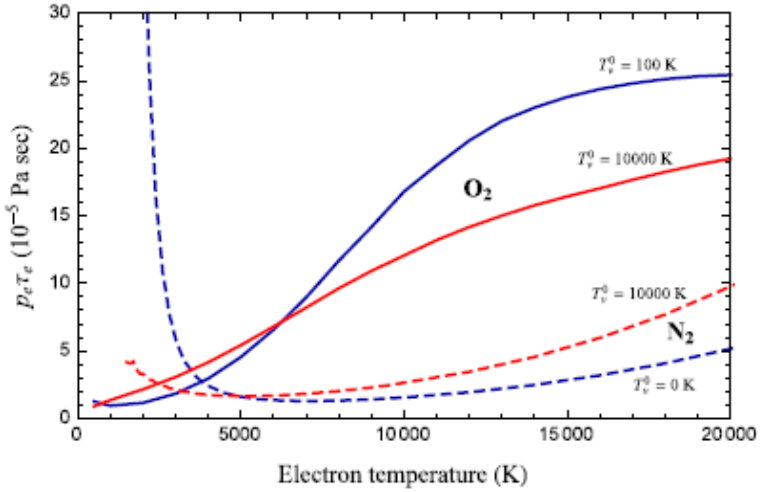

Application: non-equilibrium model for inductively coupled plasmas discharges
Preliminary results, work-in-progress

- Inductively Coupled Plasma (ICP) torches have wide range of possible applications which include deposition of metal coatings, synthesis of ultra-fine powders, generation of high purity silicon and testing of thermal protection materials for atmospheric entry vehicles;

- In the computational model, the electromagnetic induction equation is solved together with the set of Navier-Stokes equations; A state-to-state thermo-chemical non-equilibrium formulation is used for the chemical reactions;

- In its simplest configuration, an ICP torch consists of a quartz tube surrounded by an inductor coil made of a series of parallel current-carrying rings.

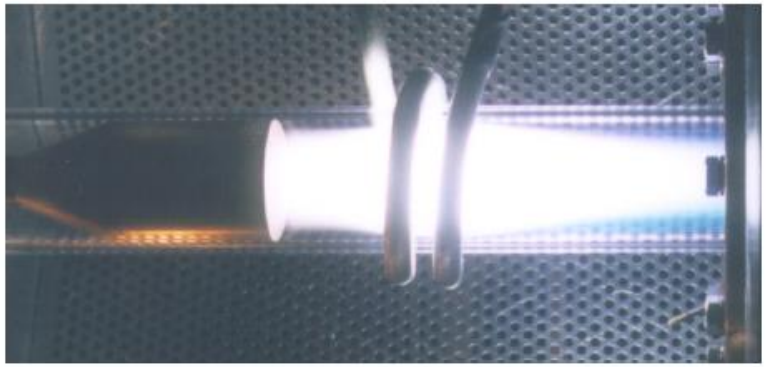

FIG. 1. Example of ICP torch in operating conditions (mini-torch facility; credits von Karman Institute for Fluid Dynamics).

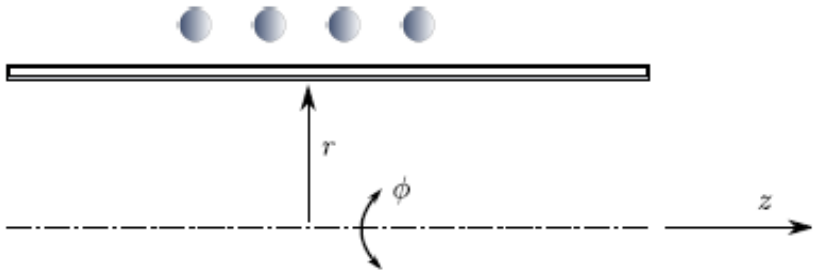

FIG. 2. Torch geometry and adopted reference frame.

$$\partial_t \rho_i + \nabla \cdot [\rho_i(\mathbf{u} + \boldsymbol{\mathcal{V}}_i)] = \mathcal{M}_i,\ \dot{\omega}_i \qquad [i \in \mathcal{S}], \qquad (2)$$

$$\partial_t(\rho \mathbf{u}) + \nabla \cdot (\rho \mathbf{u} \otimes \mathbf{u} + p\mathbb{I}) = \nabla \cdot \tau + \mathbf{J} \times \mathbf{B}, \qquad (3)$$

$$\partial_t \rho \mathcal{E} + \nabla \cdot (\rho H \mathbf{u}) + \sum_i \rho_s \boldsymbol{\mathcal{V}}_i h_i = \tau : \nabla \mathbf{u} - \nabla \cdot \mathbf{q} + \mathbf{J} \cdot \mathbf{E},$$

$$\partial_t \rho e_{ev} + \nabla \cdot (\rho e_{ev} \mathbf{u}) + \sum_i \rho_i \boldsymbol{\mathcal{V}}_i e_{ev,i}$$

$$= -\nabla \cdot \mathbf{q}_{ev} + \Omega^{ET} + \Omega^{C} + \Omega^{VT} + \mathbf{J} \cdot \mathbf{E},$$

pressure = 10^5 Pa

Power = 5 10^4 W/m

reaction	type of calculation
electron-impact excitation	
$O_2(X\,^3\Sigma, v) + e \rightleftarrows O_2(X\,^3\Sigma, w) + e$	*ab initio* RM [3, 4]
$O_2(a\,^1\Delta, v) + e \rightleftarrows O_2(a\,^1\Delta, w) + e$	scaling X state
$O_2(b\,^1\Sigma, v) + e \rightleftarrows O_2(b\,^1\Sigma, w) + e$	scaling X state
$O_2(X\,^3\Sigma, v) + e \rightleftarrows O_2(a\,^1\Delta, w) + e$	FC exp scaling
$O_2(X\,^3\Sigma, v) + e \rightleftarrows O_2(b\,^1\Sigma, w) + e$	FC exp scaling
$O_2(a\,^1\Delta, v) + e \rightleftarrows O_2(b\,^1\Sigma, w) + e$	FC exp scaling
$O(i) + e \rightleftarrows O(j) + e$	bruno [?]
heavy-particle excitation	
$O_2(X\,^3\Sigma, v) + O_2 \rightleftarrows O_2(X\,^3\Sigma, w) + O_2$	FHO [5]
$O_2(X\,^3\Sigma, v) + O(^3P) \rightleftarrows O_2(X\,^3\Sigma, w) + O(^3P)$	QCT [6]
electron-impact dissociation	
$O_2(X\,^3\Sigma, v) + e \rightleftarrows O(^3P) + O(^3P) + e$	*ab initio* RM [3, 4]
$O_2(a\,^1\Delta, v) + e \rightleftarrows O(^3P) + O(^3P) + e$	scaling X state
$O_2(b\,^1\Sigma, v) + e \rightleftarrows O(^3P) + O(^3P) + e$	scaling X state
heavy particle dissociation	
$O_2(X\,^3\Sigma, v) + O_2 \rightleftarrows O(^3P) + O(^3P) + O_2$	FHO [5]
$O_2(X\,^3\Sigma, v) + O(^3P) \rightleftarrows O(^3P) + O(^3P) + O(^3P)$	QCT [7]
ionizzation	
$O(i) + e \rightleftarrows O^+(^4S) + e + e$	Park [bruno?]
$O(^3P) + O(^3P) \rightleftarrows O_2^+(X\,^2\Pi_g) + e$	bruno [?]

Results at equilibrium:

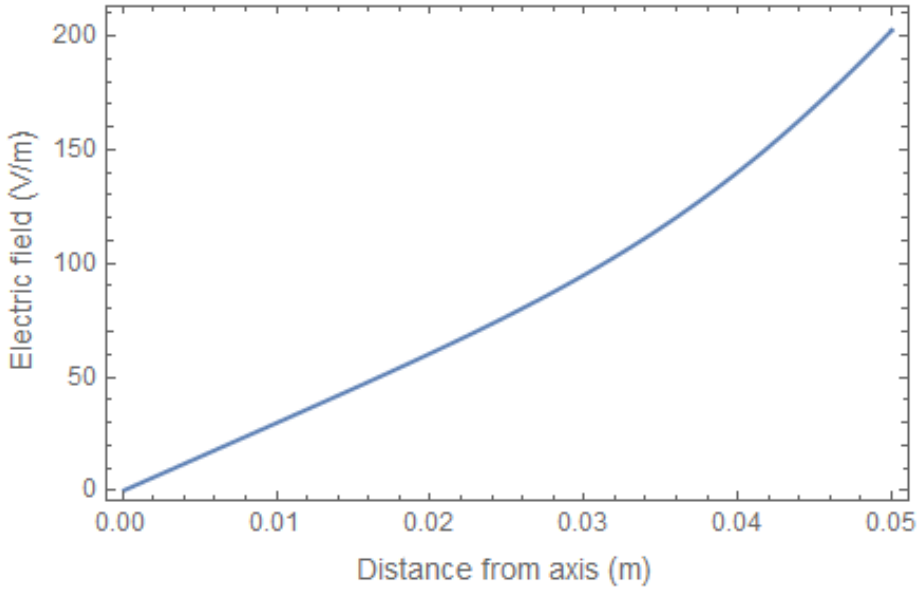

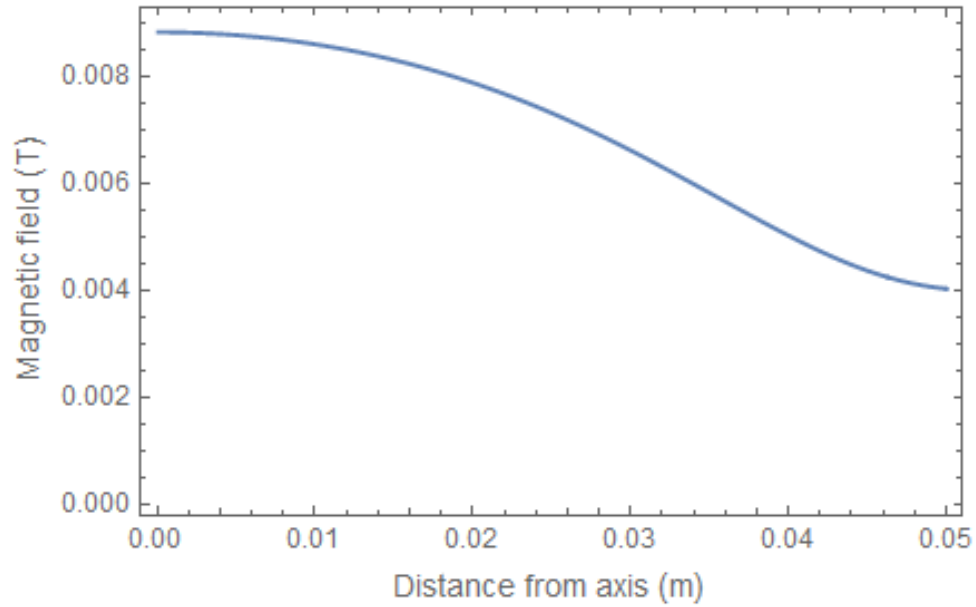

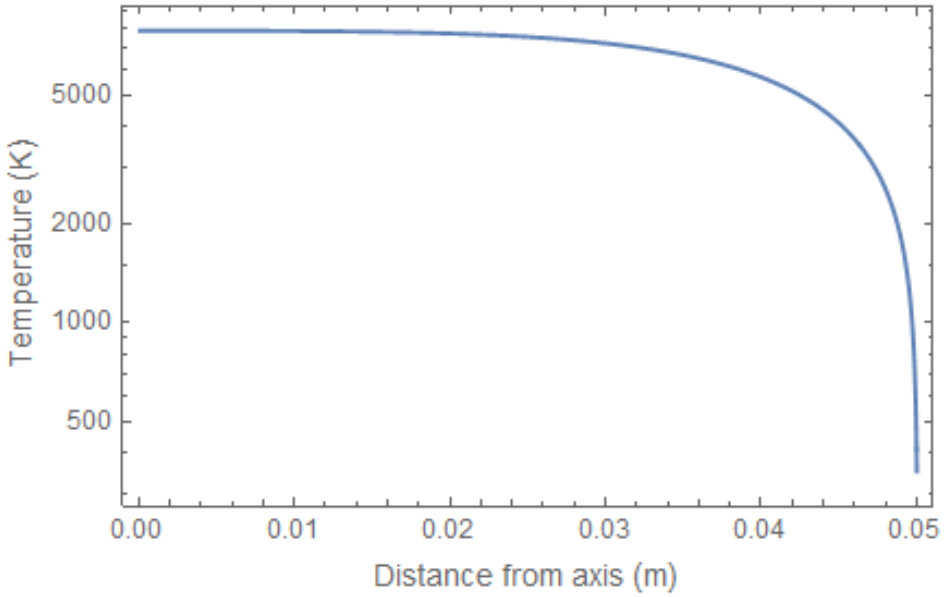

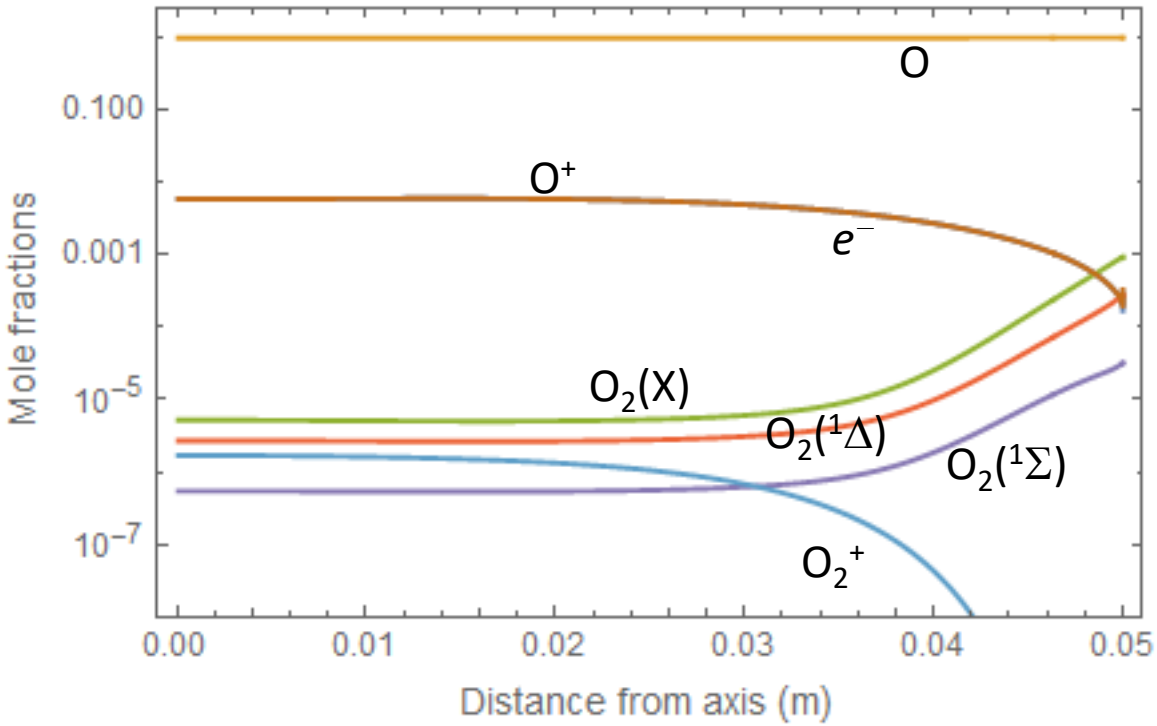
O
O+
e−
O2(X)
O2(1Δ)
O2(1Σ)
O2+
Mole fractions
0.100
0.001
10−5
10−7
0.00
0.01
0.02
0.03
0.04
0.05
Distance from axis (m)

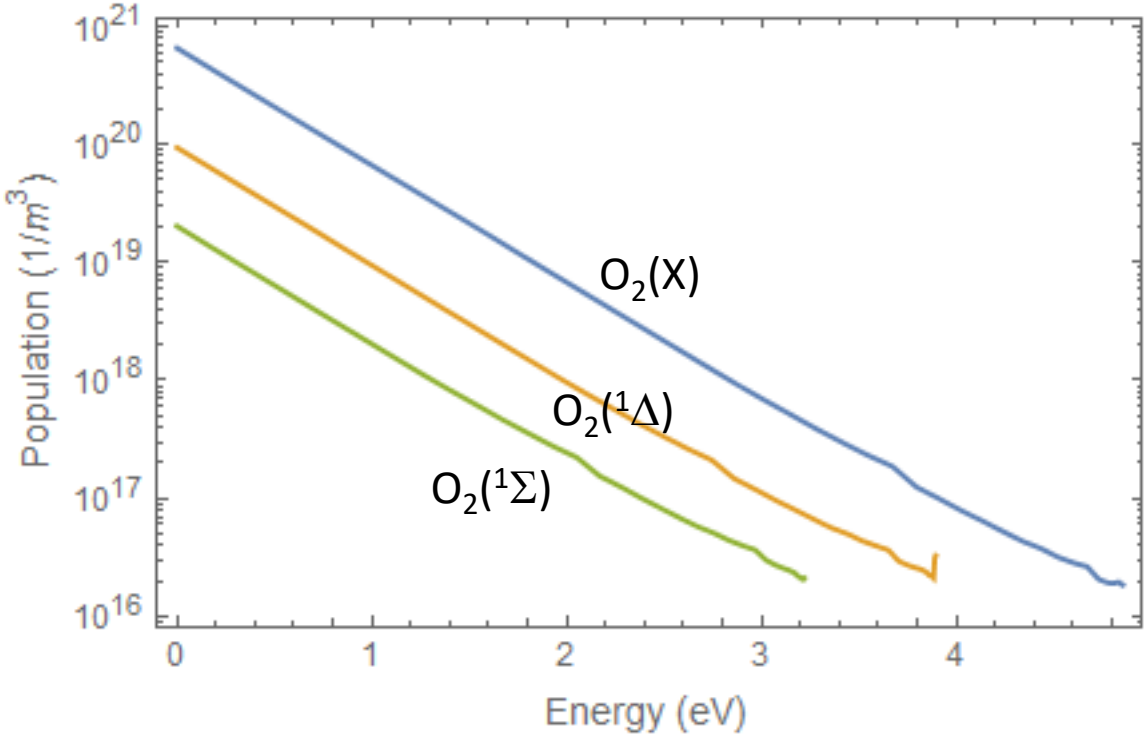
O2(X)
O2(1Δ)
O2(1Σ)
Population (1/m3)
10^21
10^20
10^19
10^18
10^17
10^16
0
1
2
3
4
Energy (eV)

Outlook...

- Complete sets, state-resolved, of vibrational-excitation, dissociative-electron-attachment and dissociative-excitation cross sections and rate coefficients for electron-oxygen scattering are supplied for plasma description purposes;

- Next step will be the updating to *ab-initio* calculations for state-resolved cross sections for excited states $^1\Delta$ and $^1\Sigma$ of oxygen;

- Calculations for electron-O_2^+ scattering for dissociative recombination process;

- Developing of a self-consistent kinetic code for inductively-coupled-plasma;

- All cross sections are available to PHYS4Entry data base:
  http://users.ba.cnr.it/imip/cscpal38/phys4entry/database.html

Thank you for your attention

Acknowledgments:

- Prof. Roberto Celiberto (Politecnico di Bari, Italy)
- Prof. Jonathan Tennyson (University College London, UK)
- Prof. Marco Panesi (University of Illinois, IL, US)
- Dr. Alessandro Munafo (University of Illinois, IL, US)